Journal of Engineering Mathematics **40:** 211–226, 2001.

On modelling an iceberg embedded in shore-fast sea ice

VERNON A. SQUIRE and TONY W. DIXON
Department of Mathematics and Statistics, University of Otago, P.O. Box 56, Dunedin, New Zealand

Received 10 December 1999; accepted in revised form 17 July 2000

Abstract. The effect of long ice-coupled waves impinging on a tabular iceberg, an ice island or a thick sea ice floe trapped within a thin veneer of shore fast sea ice of substantial extent is considered. The waves most likely originate as ocean waves in the open sea beyond the fast ice boundary, from where they propagate into the sea ice. There their character is altered because of the flexural properties of the ice. The geophysical / engineering problem posed is solved by a Green's function method that redevelops, for a different surface boundary condition, an earlier study concerned with a freely floating ice floe. Reflection and transmission coefficients for the berg are found to depend strongly on its thickness and length. Amongst other things, the work relates to the operational safety of natural and artificially thickened Arctic ice platforms located in a contiguous ice sheet.

Key words: iceberg, shore-fast sea ice, waves, Green's function, contour integration.

1. Introduction

Icebergs are formed along polar and subpolar coastlines where glaciers, ice tongues and ice shelves flow gradually into the sea. While a great variety of shapes and sizes is possible, the Antarctic tabular iceberg calved from an ice shelf is quite common, as are the so-called ice islands of the Arctic. Also in the Arctic very thick sea ice, known by the Inuit name *sikussak*, may form in sheltered areas, eventually to break out as separate floes (sometimes called floebergs), or sea ice may be artificially thickened for the purpose of supporting a drilling rig or base. Hereinafter, for convenience, we shall use the term 'berg' to designate these distinct ice types, recognizing that each type is actually fundamentally different in its origin and physical properties. At the point where the berg is created, the sea may be covered by a thin veneer of sea ice of more or less uniform thickness that is held 'fast' to the shore and can stretch for hundreds of kilometres, *e.g.* in McMurdo Sound, Antarctica, or it may be free of ice. If the water is deep enough for calved bergs not to ground immediately, these frequently massive chunks of fresh or near fresh water ice will be driven away from their source by local oceanic and meteorological forces. The presence of a surrounding sea-ice sheet does not necessarily inhibit this motion; indeed, the draft and freeboard of the berg are sufficiently different to that of the sea ice that it may cut a path through. Moreover, the berg will respond differently to the sea ice when subjected to waves.

Considerable research was done on icebergs in the late 1970s, inspired by a rather large budget that was provoked by the idea of harnessing icebergs as a fresh water source (Husseiny [1], Gold [2]). Enthusiasm waned when it became clear that the engineering challenges were just too ambitious for the time. It was demonstrated by Kristensen *et al.* [3], for example, that an Antarctic iceberg would be very unlikely to make it out of the Southern Ocean as the extreme waves there would break it up as it progressed (or was towed) north. Calculations on

melting also showed the warmer waters north of the Antarctic Convergence and Subtropical Convergence would be deleterious to the iceberg's health.

In this paper we consider how a berg that is trapped within a sheet of uniform sea ice is affected by an incoming train of waves. These waves would most likely originate in the open sea and propagate into the fast ice as described by Fox and Squire [4, 5, 6], although it is also conceivable that they could be generated by strong winds blowing over the ice sheet (Squire [7]) or even by the natural oscillations of local ice tongues (Gui and Squire [8], Squire *et al.* [9]). Waves propagating in sea ice are known either as ice-coupled waves or flexural-gravity waves, the latter term reflecting the two controlling factors that influence the way they disperse. Because shorter waves are discouraged from entering the ice sheet, the spectrum of ice-coupled waves present is generally biased towards longer periods.

There are three facets to why we have chosen to develop a solution to this problem. First, artificially thickened or natural ice islands surrounded by shore-fast sea ice are used as drilling platforms in the Arctic. Ice-coupled waves are sometimes present and may furnish an operational hazard if they are of sufficient intensity. Second, it is an interesting geophysical problem that may relate to the break-up of shore-fast sea ice and, concomitantly, to maritime transportation through ice-infested seas. Third, in the future the solution will allow us to consider wave scattering in a medium composed of a random distribution of such bergs in an ice sheet and, in the limit, scattering in pack ice.

It is assumed that the berg and its encircling sea-ice sheet floats on deep water, and that the sea ice is effectively of infinite extent. The model proposed is two-dimensional to keep the mathematics algebraically straightforward, although the extension to three dimensions should not be too problematical. (A three-dimensional Green's function equivalent to G below has been derived by Fox and Chung [10], an outcome of the same research programme as the present work.) As noted above, because the draft and freeboard of the berg is not the same as the sea-ice surrounding it, causing each to respond differently to waves, winds and currents, they are not bonded together and an open crack separates the berg from the sea-ice plate. Consequently, a free edge boundary condition holds at their respective edges, whereby bending moments and transverse shears will vanish there.

In Section 2 the model is formulated and a method of solution is described based on first finding the Green's function G for the problem with no berg present. This involves a challenging contour integration that is described in Section 2.1.1. An integral equation is then constructed by use of Green's theorem, and this is solved numerically. Finally, results are reported in Section 3, and some geophysical and engineering implications are given in Section 4.

2. Mathematical model

Consider a one-dimensional sea-ice sheet of thickness h_1 and density ρ_1 floating on deep water of density ρ. The sheet is assumed to be a thin elastic beam of infinite extent with rigidity D_1. Within the sheet floats a berg of length L, thickness h_2 and density ρ_2, also modelled as a thin elastic plate but with rigidity D_2. Physically, $h_2 > h_1$, as bergs are usually thicker than sea-ice, but the model that will be developed does not require this to be true. (Indeed, $h_1 = h_2$ is one of the tests used later to validate results.) Long-crested waves of radian frequency ω and of significant wavelength propagate towards the berg in the positive x-direction (z vertically downwards), their character being determined by the flexural properties of the sea ice in which

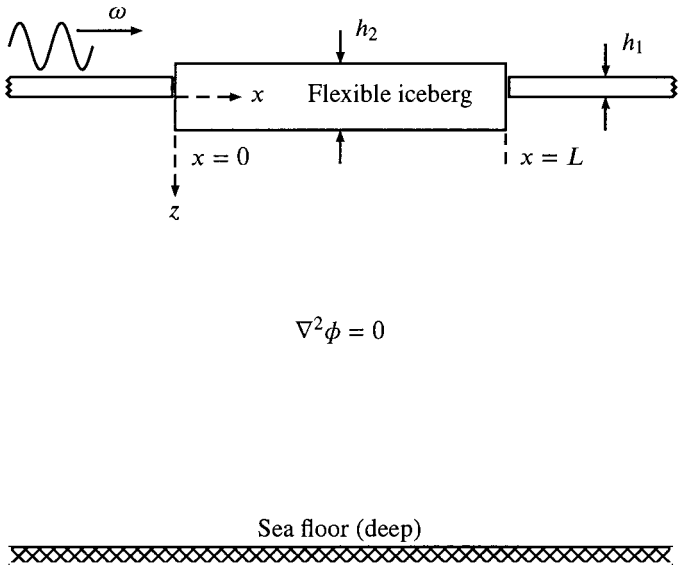

Figure 1. Schematic diagram showing the geometry of the problem and the coordinate system used. The incident wavelength is much longer than depicted here.

they travel and the inertia of the water on which it floats (see [4]). The wavelength of these waves is assumed to be much greater than h_1 and h_2. The system described is illustrated in Figure 1. That a thin-plate theory is a sufficiently good approximation to model the response of the berg, so long as the berg is not too thick, is shown by Fox and Squire [11].

In an earlier paper Meylan and Squire [12] tackle a related problem, namely a pack-ice floe subjected to a train of ocean waves. Although the problem solved herein is mathematically more demanding, the framework of [12], including its nondimensionalization, is helpful and will be repeated here. If we assume then that the velocity potential describing the system is separable and is periodic in time ($e^{-i\omega t}$), the nondimensionalized boundary-value problem we seek to solve for $\phi(x, z)$ is

$$\nabla^2\phi = 0, \quad -\infty < x < \infty, 0 < z < \infty, \tag{1a}$$

$$\beta_1 \frac{\partial^5\phi}{\partial x^4 \partial z} + (1 - \alpha\gamma_1)\frac{\partial\phi}{\partial z} + \alpha\phi = 0, \quad z = 0, -\infty < x < 0, 1 < x < \infty, \tag{1b}$$

$$\beta_2 \frac{\partial^5\phi}{\partial x^4 \partial z} + (1 - \alpha\gamma_2)\frac{\partial\phi}{\partial z} + \alpha\phi = 0, \quad z = 0, 0 \le x \le 1, \tag{1c}$$

$$\phi_z \to 0, \quad z \to \infty, \tag{1d}$$

where $\alpha = L\omega^2/g$ is the square of the nondimensionalized frequency (α is also equal to the corresponding nondimensionalized wave number in open water). The parameters $\beta_j = D_j/\rho g L^4$ and $\gamma_j = \rho_j h_j/\rho L$, $j = 1, 2$. In addition to the equations of (1) suitable radiation conditions must hold at $\pm\infty$. Note that the surface boundary conditions are applied at $z = 0$, which is consistent with the assumption that $h_1, h_2 \ll$ wavelength. While the $\alpha\gamma_j$ terms can actually be omitted in the subsequent development because of this assumption, they are retained in the equations for completeness.

2.1. THE HALF-SPACE GREEN'S FUNCTION

The method of solution we shall use first requires us to find the Green's function for the water half-space capped with a surface boundary (1b). Invoking Green's theorem in the plane, we define a Green's function $G(\xi, \zeta; x, z)$ in the usual way, *i.e.* we attempt to find a solution G of the system

$$\nabla^2 G = \delta(\xi - x)\delta(\zeta - z), \tag{2a}$$

$$\beta_1 G_{\zeta\xi\xi\xi\xi} + (1 - \alpha\gamma_1)G_\zeta + \alpha G = 0, \quad \zeta = 0, \tag{2b}$$

$$G_\zeta \to 0, \quad \zeta \to \infty, \tag{2c}$$

where $\delta(.)$ denotes the Dirac delta function. G is found most easily by using Fourier transforms, taken with respect to $x-\xi$. If we effect a change of the independent variable ξ, multiply by $\exp[ik(x - \xi)]$ and integrate over $(-\infty, \infty)$, we obtain the transformed Green's function system

$$\frac{\mathrm{d}^2\hat{G}}{\mathrm{d}\zeta^2} - k^2\hat{G} = \delta(\zeta - z), \tag{3a}$$

$$(\beta_1 k^4 + 1 - \alpha\gamma_1)\frac{\mathrm{d}\hat{G}}{\mathrm{d}\zeta} + \alpha\hat{G} = 0, \quad \zeta = 0, \tag{3b}$$

$$\frac{\mathrm{d}\hat{G}}{\mathrm{d}\zeta} \to 0, \quad \zeta \to \infty, \tag{3c}$$

where $\hat{G} = \hat{G}(k; \zeta; z)$. To arrive at (3) the boundary terms, which appear as the product of $\exp[ik(x - \xi)]$ and an expression composed of G and its derivatives, must vanish at $\pm\infty$. If this expression is chosen to be proportional to $\exp[-ik(x-\xi)]$ the offending terms vanish and we are provided with an indication of the asymptotic behaviour of G by solving the resulting inhomogeneous linear ordinary differential equation. We find that G must be proportional to $\sin k(x - \xi)$ when $(x - \xi) \to \pm\infty$, which will be verified later.

To solve (3) for $\hat{G}$ a piecewise solution of the form

$$\hat{G}(k; \zeta; z) = \begin{cases} A\mathrm{e}^{-|k|\zeta} + B\mathrm{e}^{|k|\zeta}, & 0 < \zeta < z, \\ C\mathrm{e}^{-|k|\zeta} + D\mathrm{e}^{|k|\zeta}, & z < \zeta < \infty, \end{cases} \tag{4}$$

is assumed. Using the sea-floor condition, we observe that the surface boundary condition and the usual matching conditions give

$$\hat{G}(k; \zeta; z) = -\frac{1}{2|k|}\left[\mathrm{e}^{-|k||\zeta - z|} + \left(\frac{\Lambda|k| + \alpha}{\Lambda|k| - \alpha}\right)\mathrm{e}^{-|k|(\zeta+z)}\right], \tag{5}$$

where $\Lambda = \Lambda(k) = \beta_1 k^4 + 1 - \alpha\gamma_1$. Expression (5) for $\hat{G}$ can be rearranged and then the inverse Fourier transform found, to give

$$\begin{aligned} G(\xi, \zeta; x, z) = {} & \frac{1}{4\pi}\log\left\{(\xi - x)^2 + (\zeta - z)^2\right\} - \frac{1}{4\pi}\log\left\{(\xi - x)^2 + (\zeta + z)^2\right\} \\ & - \frac{1}{2\pi}\int_{-\infty}^{\infty} \frac{\Lambda}{\Lambda|k| - \alpha}\mathrm{e}^{-|k|(\zeta+z)}\mathrm{e}^{-\mathrm{i}k(x-\xi)}\mathrm{d}k. \end{aligned} \tag{6}$$

Note that when $\beta_1 = \gamma_1 = 0$ this Green's function reduces to that for open water (Mei [13] pp. 379–383, Meylan and Squire [12]). At the surface

$$G(\xi, 0; x, z) = -\frac{1}{2\pi}\int_{-\infty}^{\infty} \frac{\Lambda}{\Lambda|k| - \alpha} \mathrm{e}^{-|k|z} \mathrm{e}^{-\mathrm{i}k(x-\xi)}\, \mathrm{d}k. \tag{7}$$

2.1.1. *Contour integration*
To continue we need to be able to numerically evaluate the expression

$$\int_{-\infty}^{\infty} \frac{\Lambda}{\Lambda|k| - \alpha} \mathrm{e}^{-|k|(\zeta+z)} \mathrm{e}^{-\mathrm{i}k(x-\xi)}\, \mathrm{d}k, \tag{8}$$

where $\Lambda = \beta_1 k^4 + 1 - \alpha\gamma_1$. Rewrite this as

$$2\mathfrak{Re}\int_{0}^{\infty} \frac{\Lambda}{\Lambda k - \alpha} \mathrm{e}^{-\mathrm{i}k[(x-\xi)-\mathrm{i}(\zeta+z)]}\, \mathrm{d}k, \tag{9}$$

where $\mathfrak{Re}$ denotes the real part; later $\mathfrak{Im}$ will be used to denote the imaginary part. Writing

$$\nu = \left(\frac{1 - \alpha\gamma_1}{\beta_1}\right)^{1/4}, \quad \sigma = \frac{\alpha}{\nu(1 - \alpha\gamma_1)},$$

and

$$X = \nu\left[(x - \xi) - \mathrm{i}(z + \zeta)\right], \quad t = \frac{k}{\nu},$$

we can simplify the integral in (9) as follows:

$$I = \int_{0}^{\infty} \frac{t^4 + 1}{t^5 + t - \sigma}\, \mathrm{e}^{-\mathrm{i}Xt}\, \mathrm{d}t. \tag{10}$$

Note that $\mathfrak{Im}(X) \leq 0$, so the integral is well defined. Partial fractions are now used to simplify the integrand in (10) to

$$\frac{t^4 + 1}{t^5 + t - \sigma} = \sum_{j=0}^{4} \frac{1}{t - a_j}\left(\frac{a_j^4 + 1}{5a_j^4 + 1}\right) = \sum_{j=0}^{4} \frac{A_j}{t - a_j}, \tag{11}$$

where the a_j are the five roots of $t^5 + t - \sigma = 0$ and $A_j = \sigma/(5\sigma - 4a_j)$. Because $\sigma > 0$ the complex roots lie in the shaded regions illustrated in Figure 2. (The notation a_j is used to denote the roots collectively, while specific roots are labelled as shown. Coefficients A_j are treated similarly.) The five roots of the original dispersion relation $\Lambda k - \alpha = 0$ are given by $k_j = \nu a_j$.

The transformation process simplifies the integration considerably, as it separates out the contributions from the positive real pole at a_0 and the two complex conjugate pairs of poles at a_+ and $\bar{a}_+$, and a_- and $\bar{a}_-$. Accordingly, integral (10) becomes

$$I = \sum_{j=0}^{4} A_j I_j = \sum_{j=0}^{4} A_j \int_{0}^{\infty} \frac{\mathrm{e}^{-\mathrm{i}Xt}}{t - a_j}\, \mathrm{d}t, \tag{12}$$

and the contribution from the integral I to $G(\xi, \zeta; x, z)$, as expressed by (6) is

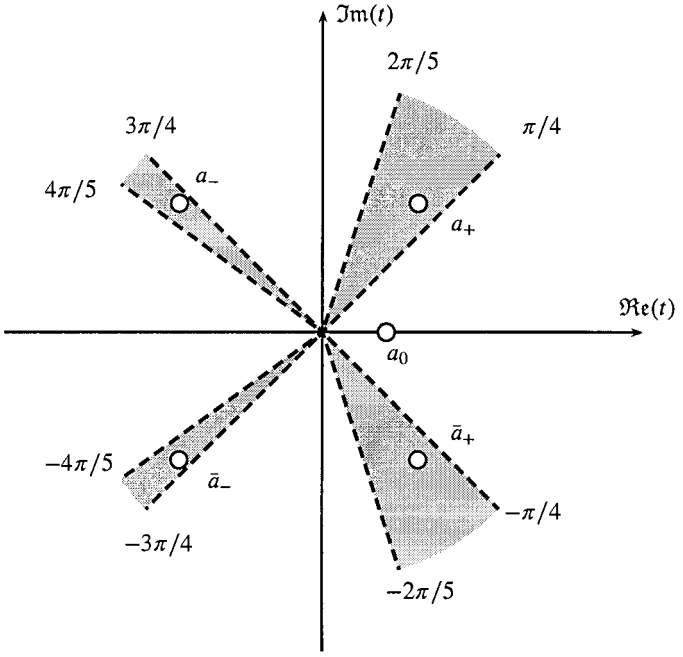

Figure 2. Zeroes of the transformed dispersion relation $t^5 + t - \sigma = 0$.

$$-\frac{1}{\pi}\Re\mathrm{e}(I) = -\frac{1}{\pi}\sum_{j=0}^{4}\Re\mathrm{e}(A_j I_j). \tag{13}$$

The explicit evaluation of (12) is done using contour integration in the lower half plane. Considerable care is necessary as five separate cases arise that depend on the value of X, if we recall that $-\pi < \arg X \leq 0$. In each case the integrals occurring on the right-hand side of (12) can be found in terms of the sine and cosine integral auxiliary functions, denoted by Abramowitz and Stegun ([14], Section 5.2) as follows:

$$f(x) = \int_0^\infty \frac{\sin w}{w+x}\mathrm{d}w, \quad g(x) = \int_0^\infty \frac{\cos w}{w+x}\mathrm{d}w, \quad \Re\mathrm{e}(x) > 0.$$

The five cases are now listed as follows:

$\Re\mathrm{e}(Xa_+) \leq 0$:

$$\begin{aligned} I \;&= A_0\left[g(-Xa_0) - \mathrm{i}f(-Xa_0) + \pi\mathrm{i}\mathrm{e}^{-\mathrm{i}Xa_0}\right] \\ &+ A_+\left[g(-Xa_+) - \mathrm{i}f(-Xa_+) + 2\pi\mathrm{i}\mathrm{e}^{-\mathrm{i}Xa_+}\right] \\ &+ \bar{A}_+\left[g(-X\bar{a}_+) - \mathrm{i}f(-X\bar{a}_+)\right] \\ &+ A_-\left[g(Xa_-) + \mathrm{i}f(Xa_-)\right] \\ &+ \bar{A}_-\left[g(X\bar{A}_-) + \mathrm{i}f(X\bar{a}_-)\right], \end{aligned} \tag{14a}$$

$\Re\mathrm{e}(X\bar{a}_+) \geq 0$:

$$
\begin{aligned}
I = \; & A_0\left[g(Xa_0) + \mathrm{i}f(Xa_0) - \pi\mathrm{i}\mathrm{e}^{-\mathrm{i}Xa_0}\right] \\
& + A_+\left[g(Xa_+) + \mathrm{i}f(Xa_+)\right] \\
& + \bar{A}_+\left[g(X\bar{a}_+) + \mathrm{i}f(X\bar{a}_+) - 2\pi\mathrm{i}\mathrm{e}^{-\mathrm{i}X\bar{a}_+}\right] \\
& + A_-\left[g(-Xa_-) - \mathrm{i}f(-Xa_-)\right] \\
& + \bar{A}_-\left[g(-X\bar{a}_-) - \mathrm{i}f(-X\bar{a}_-)\right],
\end{aligned}
\tag{14b}
$$

$\mathfrak{Re}(Xa_+) > 0, \mathfrak{Re}(X\bar{a}_+) < 0$ and $\mathfrak{Re}(X\bar{a}_-) < 0$:

$$
\begin{aligned}
I = \; & A_0\left[g(Xa_0) + \mathrm{i}f(Xa_0) - \pi\mathrm{i}\mathrm{e}^{-\mathrm{i}Xa_0}\right] \\
& + A_+\left[g(Xa_+) + \mathrm{i}f(Xa_+)\right] \\
& + \bar{A}_+\left[g(-X\bar{a}_+) - \mathrm{i}f(-X\bar{a}_+)\right] \\
& + A_-\left[g(-Xa_-) - \mathrm{i}f(-Xa_-)\right] \\
& + \bar{A}_-\left[g(-X\bar{a}_-) - \mathrm{i}f(-X\bar{a}_-)\right],
\end{aligned}
\tag{14c}
$$

$\mathfrak{Re}(Xa_+) > 0, \mathfrak{Re}(X\bar{a}_+) < 0$ and $\mathfrak{Re}(X\bar{a}_-) \geq 0$:

$$
\begin{aligned}
I = \; & A_0\left[g(-Xa_0) - \mathrm{i}f(-Xa_0) + \pi\mathrm{i}\mathrm{e}^{-\mathrm{i}Xa_0}\right] \\
& + A_+\left[g(Xa_+) + \mathrm{i}f(Xa_+)\right] \\
& + \bar{A}_+\left[g(-X\bar{a}_+) - \mathrm{i}f(-X\bar{a}_+)\right] \\
& + A_-\left[g(Xa_-) + \mathrm{i}f(Xa_-)\right] \\
& + \bar{A}_-\left[g(X\bar{a}_-) + \mathrm{i}f(X\bar{a}_-)\right],
\end{aligned}
\tag{14d}
$$

$\mathfrak{Re}(Xa_+) > 0, \mathfrak{Re}(X\bar{a}_+) < 0, \mathfrak{Re}(Xa_-) > 0$ and $\mathfrak{Re}(X\bar{a}_-) < 0$:

$$
\begin{aligned}
I = \; & A_0\left[g(-Xa_0) - \mathrm{i}f(-Xa_0) + \pi\mathrm{i}\mathrm{e}^{-\mathrm{i}Xa_0}\right] \\
& + A_+\left[g(Xa_+) + \mathrm{i}f(Xa_+)\right] \\
& + \bar{A}_+\left[g(X\bar{a}_+) + \mathrm{i}f(X\bar{a}_+)\right] \\
& + A_-\left[g(Xa_-) + \mathrm{i}f(Xa_-)\right] \\
& + \bar{A}_-\left[g(-X\bar{a}_-) - \mathrm{i}f(-X\bar{a}_-)\right].
\end{aligned}
\tag{14d}
$$

Having evaluated (10), we now know expression (6) for $G(\xi, \zeta; x, z)$ in terms of functions whose properties are understood and tabulated ([14], Chapter 5).

In the limit as $x \to \pm\infty$, the real pole will dominate the asymptotic behaviour of the Green's function. Since for large positive $\mathfrak{Re}(X)$,

$$I \sim -A_0\pi \mathrm{i} \mathrm{e}^{-\mathrm{i}Xa_0} + \frac{\mathrm{i}}{\sigma X} + O(\frac{1}{X^2}), \tag{15}$$

we find

$$\lim_{x\to\pm\infty} G(\xi,\zeta;x,z) = \pm A_0 \mathrm{e}^{-k_0(\zeta+z)} \sin k_0(x-\xi). \tag{16}$$

Hence,

$$\lim_{\xi\to\pm\infty} G(\xi,\zeta;x,z) = \pm A_0 \mathrm{e}^{-k_0(\zeta+z)} \sin k_0(\xi-x), \tag{17a}$$

$$\lim_{\xi\to\pm\infty} G_\xi(\xi,\zeta;x,z) = \pm k_0 A_0 \mathrm{e}^{-k_0(\zeta+z)} \cos k_0(\xi-x), \tag{17b}$$

$$\lim_{\xi\to\pm\infty} G_\zeta(\xi,\zeta;x,z) = -k_0 G(\xi,\zeta;x,z). \tag{17c}$$

2.2. The iceberg Green's function

The boundary condition (1c) beneath the iceberg for $z = 0$ can be rewritten as

$$\frac{\mathrm{d}^4\phi_z}{\mathrm{d}x^4} - \mu^4\phi_z = -\frac{\alpha}{\beta_2}\phi, \quad z = 0,\ 0 \le x \le 1, \tag{18}$$

where $\mu^4 = (\alpha\gamma_2 - 1)/\beta_2$. The usual free-edge boundary conditions hold at the ends of the iceberg, namely

$$\left.\frac{\mathrm{d}^2\phi_z}{\mathrm{d}x^2}\right|_{x=0} = \left.\frac{\mathrm{d}^2\phi_z}{\mathrm{d}x^2}\right|_{x=1} = 0, \quad \left.\frac{\mathrm{d}^3\phi_z}{\mathrm{d}x^3}\right|_{x=0} = \left.\frac{\mathrm{d}^3\phi_z}{\mathrm{d}x^3}\right|_{x=1} = 0. \tag{19}$$

Following Meylan and Squire [12] we can construct a Green's function $g(\xi, x)$ to enable us to replace (18) and (19) with an integral equation for ϕ_z at the surface; $g(\xi, x)$ satisfies

$$\frac{\mathrm{d}^4 g(\xi,x)}{\mathrm{d}\xi^4} - \mu^4 g(\xi,x) = \delta(\xi - x), \tag{20}$$

together with the boundary conditions

$$g_{\xi\xi}(0,x) = g_{\xi\xi}(1,x) = g_{\xi\xi\xi}(0,x) = g_{\xi\xi\xi}(1,x) = 0.$$

The general solution of (20) can be expressed in piecewise form

$$\frac{\alpha}{\beta_2} g(\xi,x) = \begin{cases} A_1\mathrm{e}^{\mathrm{i}\mu\xi} + B_1\mathrm{e}^{-\mathrm{i}\mu\xi} + C_1\mathrm{e}^{\mu\xi} + D_1\mathrm{e}^{-\mu\xi}, & 0 < \xi < x < 1, \\ A_2\mathrm{e}^{\mathrm{i}\mu\xi} + B_2\mathrm{e}^{-\mathrm{i}\mu\xi} + C_2\mathrm{e}^{\mu\xi} + D_2\mathrm{e}^{-\mu\xi}, & 0 < x < \xi < 1. \end{cases}$$

If we now apply the end conditions together with the matching and jump conditions at $\xi = x$, we can show that the following matrix equation for the unknown coefficient functions must hold:

$$\begin{pmatrix} -1 & -1 & 1 & 1 \\ -\mathrm{i} & \mathrm{i} & 1 & -1 \\ -\mathrm{e}^{\mathrm{i}\mu} & -\mathrm{e}^{-\mathrm{i}\mu} & \mathrm{e}^{\mu} & \mathrm{e}^{-\mu} \\ -\mathrm{i}\mathrm{e}^{\mathrm{i}\mu} & \mathrm{i}\mathrm{e}^{-\mathrm{i}\mu} & \mathrm{e}^{\mu} & -\mathrm{e}^{-\mu} \end{pmatrix} \begin{pmatrix} A_1 \\ B_1 \\ C_1 \\ D_1 \end{pmatrix} = -\frac{\alpha}{2\beta_2\mu^3} \begin{pmatrix} 0 \\ 0 \\ \sin\mu(1-x) + \sinh\mu(1-x) \\ \cos\mu(1-x) + \cosh\mu(1-x) \end{pmatrix},$$

where the remaining coefficients are given by

$$A_2 = A_1 + \frac{\mathrm{i}\alpha}{4\beta_2\mu^3}\mathrm{e}^{-\mathrm{i}\mu x}, \quad B_2 = B_1 - \frac{\mathrm{i}\alpha}{4\beta_2\mu^3}\mathrm{e}^{\mathrm{i}\mu x},$$
$$C_2 = C_1 + \frac{\alpha}{4\beta_2\mu^3}\mathrm{e}^{-\mu x}, \quad D_2 = D_1 - \frac{\alpha}{4\beta_2\mu^3}\mathrm{e}^{\mu x}.$$

Then, $\phi_z(x, 0)$ can be obtained by integrating over the berg to give

$$\phi_z(x, 0) = -\frac{\alpha}{\beta_2}\int_0^1 g(\xi, x)\phi(\xi, 0)\mathrm{d}\xi, \qquad z = 0,\ 0 < x < 1. \tag{21}$$

2.3. Formulation of integral equation

Green's theorem in the plane is now applied to the rectangle Γ with sides $\xi = -\xi_0$, $\xi = \xi_0$, $\zeta = 0$, $\zeta = \zeta_0$ where ξ_0 and ζ_0 are taken to be sufficiently large to include the point (x, z). Denoting differentiation with respect to the outward normal by subscript n, we have

$$\phi(x, z) = \int_\Gamma (\phi G_n - \phi_n G)\ \mathrm{d}s. \tag{22}$$

Because

$$\lim_{\xi\to+\infty}\phi(\xi, \zeta) = T\mathrm{e}^{\mathrm{i}k_0\xi - k_0\zeta}, \tag{23a}$$

$$\lim_{\xi\to-\infty}\phi(\xi, \zeta) = \mathrm{e}^{\mathrm{i}k_0\xi - k_0\zeta} + R\mathrm{e}^{-\mathrm{i}k_0\xi - k_0\zeta}, \tag{23b}$$

we have

$$\lim_{\xi_0\to+\infty}\int_0^\infty (\phi G_n - \phi_n G)|_{\xi=\xi_0}\,\mathrm{d}\zeta = \frac{1}{2}A_0 T\mathrm{e}^{\mathrm{i}k_0 x}\mathrm{e}^{-k_0 z}, \tag{24a}$$

$$\lim_{\xi_0\to-\infty}\int_0^\infty (\phi G_n - \phi_n G)|_{\xi=\xi_0}\,\mathrm{d}\zeta = \frac{1}{2}A_0(\mathrm{e}^{\mathrm{i}k_0 x} + R\mathrm{e}^{-\mathrm{i}k_0 x})\mathrm{e}^{-k_0 z}. \tag{24b}$$

It now only remains to consider (22) at $\zeta = \zeta_0 \to \infty$, which vanishes as ϕ_n and G_n are both defined to be zero there, and at $\zeta = 0$. In the latter case we must distinguish three subintegrals, namely from $-\infty$ to 0, from 0 to 1, and from 1 to ∞. If we use the surface boundary condition (1b), we may write (22) for the integration over $[1, \infty)$, for example,

$$\begin{aligned}\textstyle\int_1^\infty(\phi G_n - \phi_n G)\mathrm{d}\xi &= \tfrac{\beta_1}{\alpha}\textstyle\int_1^\infty(\phi_{\zeta\xi\xi\xi\xi}G_\zeta - G_{\zeta\xi\xi\xi\xi}\phi_\zeta)\ \mathrm{d}\xi \\ &= \frac{\beta_1}{\alpha}\left[\phi_{\zeta\xi\xi\xi}G_\zeta - \phi_{\zeta\xi\xi}G_{\zeta\xi} + \phi_{\zeta\xi}G_{\zeta\xi\xi} - \phi_\zeta G_{\zeta\xi\xi\xi}\right]_1^\infty,\end{aligned} \tag{25}$$

at $\zeta = 0$. Consider first the upper $(+\infty)$ limit. Here we know the form of ϕ and G and their relevant derivatives from (17) and (23). Substitution produces a contribution

$$\frac{2TA_0\beta_1 k_0^5}{\alpha}\mathrm{e}^{\mathrm{i}k_0 x}\mathrm{e}^{-k_0 z},$$

which combines with result (24a) to give a total contribution at $+\infty$ of

$$\tfrac{1}{2}T\mathrm{e}^{\mathrm{i}k_0x}\mathrm{e}^{-k_0z}. \tag{26}$$

In similar fashion the lower $(-\infty)$ limit of the integral from $-\infty$ to 0 associates with (24b) to give

$$\frac{1}{2}(\mathrm{e}^{\mathrm{i}k_0x} + R\mathrm{e}^{-\mathrm{i}k_0x})\mathrm{e}^{-k_0z}. \tag{27}$$

We may now write out the integral equation for $\phi(x, z)$ as follows

$$\begin{aligned}\phi(x,z) = {} & \frac{1}{2}\left[(1+T)\mathrm{e}^{\mathrm{i}k_0x} + R\mathrm{e}^{-\mathrm{i}k_0x}\right]\mathrm{e}^{-k_0z} \\ & + \frac{\beta_1}{\alpha}\left[\phi_{\zeta\xi}(0,0)G_{\zeta\xi\xi}(0,0;x,z) - \phi_{\zeta}(0,0)G_{\zeta\xi\xi\xi}(0,0;x,z)\right] \\ & - \frac{\beta_1}{\alpha}\left[\phi_{\zeta\xi}(1,0)G_{\zeta\xi\xi}(1,0;x,z) - \phi_{\zeta}(1,0)G_{\zeta\xi\xi\xi}(1,0;x,z)\right] \\ & + \int_0^1 \left[G(\xi,0;x,z)\phi_{\zeta}(\xi,0) - G_{\zeta}(\xi,0;x,z)\phi(\xi,0)\right]\mathrm{d}\xi,\end{aligned} \tag{28}$$

where the free-edge boundary conditions (19) have been used. Hence, on $z = 0$

$$\begin{aligned}\phi(x,0) = {} & \frac{1}{2}\left[(1+T)\mathrm{e}^{\mathrm{i}k_0x} + R\mathrm{e}^{-\mathrm{i}k_0x}\right] \\ & + \frac{\beta_1}{\alpha}\left[\phi_{\zeta\xi}(0,0)G_{\zeta\xi\xi}(0,0;x,0) - \phi_{\zeta}(0,0)G_{\zeta\xi\xi\xi}(0,0;x,0)\right] \\ & - \frac{\beta_1}{\alpha}\left[\phi_{\zeta\xi}(1,0)G_{\zeta\xi\xi}(1,0;x,0) - \phi_{\zeta}(1,0)G_{\zeta\xi\xi\xi}(1,0;x,0)\right] \\ & + \int_0^1 \left[G(\xi,0;x,0)\phi_{\zeta}(\xi,0) - G_{\zeta}(\xi,0;x,0)\phi(\xi,0)\right]\mathrm{d}\xi.\end{aligned} \tag{29}$$

Expression (29) allows the reflection and transmission coefficients, R and T, respectively, to be found by considering either $x \to \infty$ or $x \to -\infty$, each giving the same result. First we write the asymptotic forms of G, G_{ζ}, $G_{\zeta\xi\xi}$ and $G_{\zeta\xi\xi\xi}$ for $\zeta = z = 0$ as $x \to \infty$ in terms of the linearly independent functions $\mathrm{e}^{\mathrm{i}k_0x}$ and $\mathrm{e}^{-\mathrm{i}k_0x}$. Then we compare the coefficients of these functions, to obtain

$$\begin{aligned}R = {} & -\frac{A_0\beta_1k_0^3}{\alpha}\left\{\left[\mathrm{i}\phi_{\zeta\xi}(0,0) + k_0\phi_{\zeta}(0,0)\right] - \mathrm{e}^{\mathrm{i}k_0}\left[\mathrm{i}\phi_{\zeta\xi}(1,0) + k_0\phi_{\zeta}(1,0)\right]\right\} \\ & -\mathrm{i}A_0\textstyle\int_0^1 \mathrm{e}^{\mathrm{i}k_0\xi}\left[k_0\phi(\xi,0)_{+}\phi_{\zeta}(\xi,0)\right]\mathrm{d}\xi,\end{aligned} \tag{30a}$$

$$\begin{aligned}T = {} & 1 - \frac{A_0\beta_1k_0^3}{\alpha}\left\{\left[\mathrm{i}\phi_{\zeta\xi}(0,0) - k_0\phi_{\zeta}(0,0)\right] - \mathrm{e}^{-\mathrm{i}k_0}\left[\mathrm{i}\phi_{\zeta\xi}(1,0) - k_0\phi_{\zeta}(1,0)\right]\right\} \\ & -\mathrm{i}A_0\textstyle\int_0^1 \mathrm{e}^{-\mathrm{i}k_0\xi}\left[k_0\phi(\xi,0)_{+}\phi_{\zeta}(\xi,0)\right]\mathrm{d}\xi.\end{aligned} \tag{30b}$$

Resubstitution in (28) finally gives an integral equation for ϕ

$$
\begin{aligned}
\phi(x,z) &= \mathrm{e}^{\mathrm{i}k_0 x - k_0 z} \\
&-\frac{\beta_1}{\alpha}\phi_{\zeta\xi}(0,0)\Big[\mathrm{i}A_0 k_0^3 \mathrm{e}^{-k_0 z}\cos k_0 x - G_{\zeta\xi\xi}(0,0;x,z)\Big] \\
&+\frac{\beta_1}{\alpha}\phi_{\zeta}(0,0)\Big[\mathrm{i}A_0 k_0^4 \mathrm{e}^{-k_0 z}\sin k_0 x - G_{\zeta\xi\xi\xi}(0,0;x,z)\Big] \\
&+\frac{\beta_1}{\alpha}\phi_{\zeta\xi}(1,0)\Big[\mathrm{i}A_0 k_0^3 \mathrm{e}^{-k_0 z}\cos k_0 (x-1) - G_{\zeta\xi\xi}(1,0;x,z)\Big] \\
&-\frac{\beta_1}{\alpha}\phi_{\zeta}(1,0)\Big[\mathrm{i}A_0 k_0^4 \mathrm{e}^{-k_0 z}\sin k_0 (x-1) - G_{\zeta\xi\xi\xi}(1,0;x,z)\Big] \\
&-\mathrm{i}A_0 \mathrm{e}^{-k_0 z}\int_0^1 \cos k_0(\xi - x)\Big[k_0\phi(\xi,0) + \phi_\zeta(\xi,0)\Big]\,\mathrm{d}\xi \\
&+\int_0^1 \Big[G(\xi,0;x,z)\phi_\zeta(\xi,0) - G_\zeta(\xi,0;x,z)\phi(\xi,0)\Big]\,\mathrm{d}\xi.
\end{aligned}
\tag{31}
$$

The integral equation (31) still has four unknowns, namely $\phi_{\zeta\xi}$ and ϕ_ζ on $\zeta = 0$ at $\xi = 0$ and 1. To find these we must apply the adjoint boundary conditions $\phi_{zxx}(0,0) = \phi_{zxxx}(0,0) = 0$ and $\phi_{zxx}(1,0) = \phi_{zxxx}(1,0) = 0$. This is done by first differentiating (31) formally to obtain $\phi_{zxx}(x,z)$ and $\phi_{zxxx}(x,z)$, then taking the limit $z \to 0$ using the known behaviour of the sine and cosine integral auxiliary functions for small arguments ([14], Section 5.2), and finally evaluating the results at $x = 0$ and $x = 1$. Fortunately, potentially singular contributions in the derivatives of the Green's function vanish, either in the process of taking the real part or because the roots a_j of $t^5 + t - \sigma = 0$ satisfy certain conditions, which in terms of k_j are

$$
\sum_{j=0}^{4} A_j = 1, \sum_{j=0}^{4} A_j k_j = \sum_{j=0}^{4} A_j k_j^2 = \sum_{j=0}^{4} A_j k_j^3 = \sum_{j=0}^{4} A_j k_j^4 = 0.
$$

Similar expressions for higher powers of k_j then follow from $a_j^5 = \sigma - a_j$. In particular, we find that $G(\xi,0;x,0)$ is the *only* singular kernel as $|\xi - x| \to 0$. Because G is symmetric about $\xi = x$, differentiating an odd number of times in ξ and x combined yields an antisymmetric function. Differentiation with respect to ζ or z does not alter this symmetry.

Given four equations in four unknowns, we may write down a matrix equation for the boundary terms, as follows:

$$
\mathbf{M}\begin{bmatrix} \phi_{\zeta\xi}(0,0) \\ \phi_\zeta(0,0) \\ \phi_{\zeta\xi}(1,0) \\ \phi_\zeta(1,0) \end{bmatrix} = \boldsymbol{C} + \int_0^1 \boldsymbol{P}(\xi)\phi(\xi,0)\mathrm{d}\xi + \int_0^1 \boldsymbol{Q}(\xi)\phi_\zeta(\xi,0)\mathrm{d}\xi. \tag{32}
$$

In this equation $\mathbf{M}$ is composed of real and imaginary parts, $\mathbf{M_r}$ and $\mathbf{M_i}$, that may be written

$$\mathbf{M_r} = \frac{\beta_1}{\alpha} \times$$

$$\begin{bmatrix} G_{\zeta\xi\xi zxx}(0;0) & -G_{\zeta\xi\xi\xi zxx}(0;0) & -G_{\zeta\xi\xi zxx}(1;0) & G_{\zeta\xi\xi\xi zxx}(1;0) \\ G_{\zeta\xi\xi zxxx}(0;0) & -G_{\zeta\xi\xi\xi zxxx}(0;0) & -G_{\zeta\xi\xi zxxx}(1;0) & G_{\zeta\xi\xi\xi zxxx}(1;0) \\ G_{\zeta\xi\xi zxx}(0;1) & -G_{\zeta\xi\xi\xi zxx}(0;1) & -G_{\zeta\xi\xi zxx}(1;1) & G_{\zeta\xi\xi\xi zxx}(1;1) \\ G_{\zeta\xi\xi zxxx}(0;1) & -G_{\zeta\xi\xi\xi zxxx}(0;1) & -G_{\zeta\xi\xi zxxx}(1;1) & G_{\zeta\xi\xi\xi zxxx}(1;1) \end{bmatrix},$$

where $G(\xi; x)$ denotes $G(\xi, 0; x, 0)$, and

$$\mathbf{M_i} = \frac{\beta_1 A_0 k_0^6}{\alpha} \begin{bmatrix} -1 & 0 & \cos k_0 & k_0 \sin k_0 \\ 0 & k_0^2 & k_0 \sin k_0 & -k_0^2 \cos k_0 \\ -\cos k_0 & k_0 \sin k_0 & 1 & 0 \\ k_0 \sin k_0 & k_0^2 \cos k_0 & 0 & -k_0^2 \end{bmatrix}.$$

Note that the antisymmetric functions in $\mathbf{M_r}$ with $\xi = x$, *i.e.* those with an odd total number of differentiations in ξ and x, are zero, matching the zero terms in $\mathbf{M_i}$. The remaining vectors are

$$\boldsymbol{C} = -k_0^3 \begin{bmatrix} 1 \\ \mathrm{i}k_0 \\ \mathrm{e}^{\mathrm{i}k_0} \\ \mathrm{i}k_0 \mathrm{e}^{\mathrm{i}k_0} \end{bmatrix},$$

$$\boldsymbol{P} = \boldsymbol{P_r} + \mathrm{i}\boldsymbol{P_i} = \begin{bmatrix} G_{\zeta zxx}(\xi;0) \\ G_{\zeta zxxx}(\xi;0) \\ G_{\zeta zxx}(\xi;1) \\ G_{\zeta zxxx}(\xi;1) \end{bmatrix} + \mathrm{i}A_0 k_0^4 \begin{bmatrix} \cos k_0 \xi \\ k_0 \sin k_0 \xi \\ \cos k_0(\xi - 1) \\ k_0 \sin k_0(\xi - 1) \end{bmatrix},$$

and

$$\boldsymbol{Q} = \boldsymbol{Q_r} + \mathrm{i}\boldsymbol{Q_i} = -\begin{bmatrix} G_{zxx}(\xi;0) \\ G_{zxxx}(\xi;0) \\ G_{zxx}(\xi;1) \\ G_{zxxx}(\xi;1) \end{bmatrix} + \mathrm{i}A_0 k_0^3 \begin{bmatrix} \cos k_0 \xi \\ k_0 \sin k_0 \xi \\ \cos k_0(\xi - 1) \\ k_0 \sin k_0(\xi - 1) \end{bmatrix}.$$

Premultiplying (32) by the inverse of $\mathbf{M}$, we can express the boundary terms as sums of integrals involving the unknown functions ϕ and ϕ_ζ. Equations (32) and (31) together with (21) allow us to solve for $\phi(x, z)$ numerically using the quadrature or Nystrom method.

3. Results

The validity of the theory derived in the preceding section and its numerical implementation can be checked in several ways, as follows:

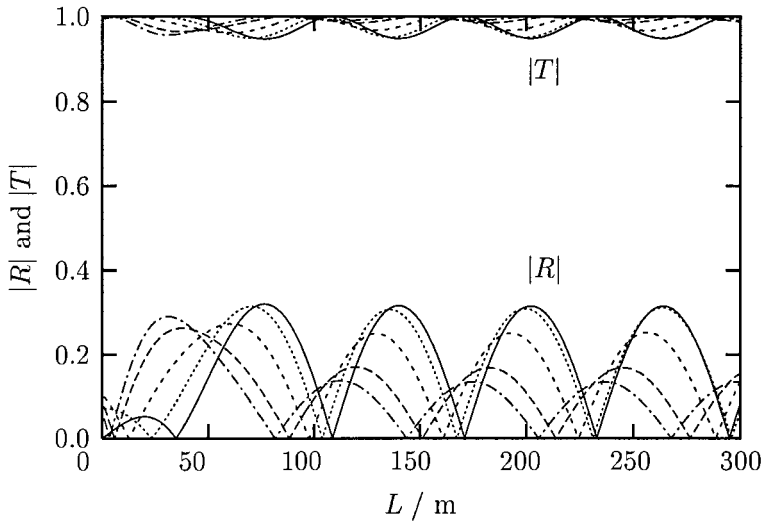

Figure 3. The magnitude of the reflection and transmission coefficients, $|R|$ and $|T|$, as a function of the berg's length for a wavelength of 100 m. The (solid) upper $|R|$ bounding curve corresponds to the solution of Meylan and Squire [12], the dotted curve has $h_1 = 0{\cdot}5$, $h_2 = 1$, the short dashed curve has $h_1 = 0{\cdot}7$, $h_2 = 1$, the long dashed curve has $h_1 = 0{\cdot}9$, $h_2 = 1$, and the (chained) lower curve is the solution for a uniform ice sheet with two parallel cracks L apart ($h_1 = h_2 = 1$). The $|T|$ curves, which satisfy $|R|^2 + |T|^2 = 1$, will not be discussed explicitly in the text.

1. an energy flux argument can be used to demonstrate that $|R|^2 + |T|^2 = 1$, which can be verified in the computed results;

2. values of β_1, γ_1 and β_2, γ_2 can be chosen such that the results of Meylan and Squire [12] are replicated, *i.e.* the thickness of the surrounding sea ice, h_1, can be made much thinner than the berg's thickness, h_2, approximating open water;

3. h_1 and h_2 can be set equal, with the result that the integral equation (31) reverts to a linear system of algebraic equations that can be solved more straightforwardly (Squire and Dixon [15]).

The results we present satisfy $|R|^2 + |T|^2 = 1$ to a high order of accuracy. That they also confirm 2 and 3 above is shown in Figure 3. Focusing on the lower part of the figure without loss of generality, *i.e.* on $|R|$, we see a set of five curves for the reflection coefficient that all exhibit a similar structure. The solid curve describes the behaviour when the sea ice surrounding the berg is replaced with open water, *i.e.* the solution of Meylan and Squire [12]. The chained curve illustrates no change of thickness between the surrounding sea ice and the berg, *i.e.* the solution corresponds to a pair of cracks in an otherwise featureless and uniform sea ice sheet. The intermediate curves are included to show how the latter solution for constant thickness [15] converges onto the Meylan and Squire solution as the sea ice thickness $h_1 \to 0$. It is apparent that the reflection coefficient approaches the open water solution as h_1 is decreased; indeed, the (dotted) curve corresponding to $h_1 = 0{\cdot}5$ is already quite close. A further similar decrease in h_1 yields a curve that is indistinguishable (in the plot) from the open water curve. Reduction of h_1 to very small values reproduces the results of [12] with a high degree of accuracy and stability.

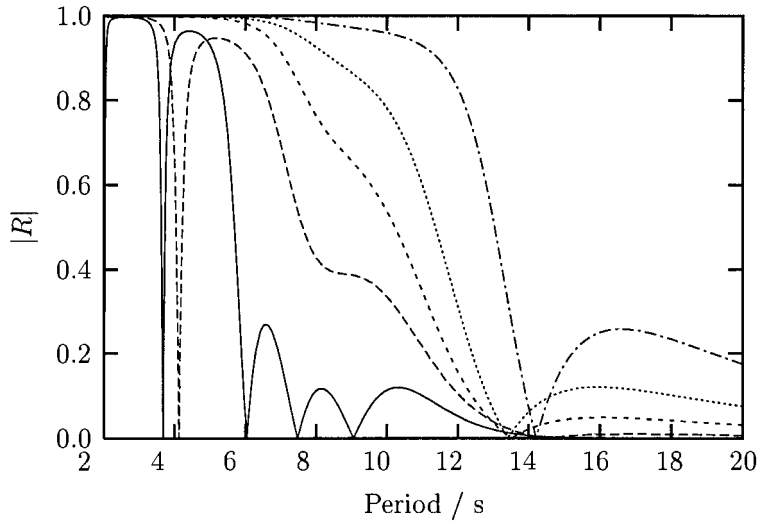

Figure 4. The magnitude of the reflection coefficient $|R|$ plotted against wave period for a berg of length 100 m and thickness (i) 1 m (solid), (ii) 2 m (long dashed), (iii) 5 m (short dashed), (iv) 10 m (dotted), and (v) 20 m (chained) embedded in sea ice of thickness $h_1 = 1$.

Each reflection coefficient curve in Figure 3 has the same generic structure, namely, a series of smooth, concave-down segments separated by zeros that we shall loosely call 'resonances'. The distance between adjacent zeros becomes constant, as does the height of the peak, once the length of the berg has exceeded one or two wavelengths. Closer to $L = 0$ the curves are less systematic. The observed resonances where perfect transmission occurs are similar to those that arise when electromagnetic waves propagate through an homogeneous slab. Nonetheless, they are interesting geophysically, as they suggest that bergs will be invisible to ice-coupled waves at some periods, *cf.* solitary ice floes in open water [12].

While Figure 3 establishes the validity of the theory and associated numerical solution, it does not present the results of the calculation in the most natural way. This is done in Figure 4 for bergs of different thickness trapped in 1 m thick sea ice. In the case of the solid curve, where $h_1 = h_2 = 1$, the solution has been computed using integral equation (31) rather than the simpler method described in [15], as a further check. The relevant curve of Figure 4, drawn solid, is found to be indistinguishable from the one appearing in the appropriate figure of [15].

The curves of Figure 4 may be described generically as a low pass filter but in each case the aforementioned resonances, where $|R| = 0$ and transmission is perfect, may occur at certain periods. These points occur where the real and imaginary parts of R intersect at 0, *i.e.* at the centre point of a 2π phase change in arg R. The effect of increasing the thickness of the berg is to shift the transition band of the filter to the right towards longer periods and to decrease the number of times the reflection coefficient drops to zero. Resonances are consequently most common in the uniform cracked sheet of constant thickness.

Recall that the model requires h_1 and h_2 to be small compared to the wavelength. This is because of the overarching assumption that the beam is thin and because of submergence, although the former condition has been shown to not be too strict in [11]. Submergence will play a role, if it is noted that bergs typically have drafts that are several times their freeboards, and it is for this reason that we have restricted the example to thicknesses less

than 20 m. However, it is also true that reflection will be complete for waves that are affected by submergence and this is actually what the model has predicted.

4. Conclusions

We have derived an analytical model to describe wave propagation through uniform sea ice in which an unattached berg of some kind is embedded. Concomitantly, the model can solve the equivalent problem of what happens when waves encounter two cracks in an otherwise featureless ice sheet. We have validated the model and its numerical solution by using [12] and [15], which, respectively, consider a related problem for open water and report a direct solution of the two-crack problem.

It is found that reflection is strongly dependent on wave period; within a low-pass filter structure a number of zeros occur that correspond to perfect transmission. The filter's transition band is positioned according to the thickness of the berg.

The results have important consequences to the breakup of icebergs and ice islands, as they suggest that breakup can take place even when the berg is protected from intense open water waves by a thinner veneer of sea ice. The same is true of ice platforms that have been artificially thickened for hydrocarbon exploration. The reason for this is twofold. First, the low pass filter for cracked sea ice of uniform thickness removes only very short waves. Second, the presence of cracks in an otherwise uniform ice plate induces perfect transmission at some periods, the comb of points at which $|R| = 0$ becoming finer as the number of cracks per unit length is increased [15] because it depends on crack separation in relation to wavelength. Accordingly, ice-coupled waves may still be present with sufficient magnitude to do damage.

Acknowledgements

The bulk of the work described in this paper was funded by a Marsden Grant administered by the Royal Society of New Zealand, with additional support from the New Zealand Public Good Science Fund and the University of Otago. We are very grateful to Dr Peter Fenton who assisted us considerably with the evaluation of the integral appearing in the Green's function (6).

References

1. A. A. Husseiny (ed.), *Proc. 1st Int. Conf. on Iceberg Utilization.* New York: Pergamon Press (1977) 760 pp.
2. L. W. Gold (ed.), *Use of Icebergs: Scientific and Practical Feasibility. Proc. 2nd Int. Conf., Ann. Glaciol.* 1 (1980) 136 pp.
3. M. Kristensen, V. A. Squire and S. C. Moore, Tabular icebergs in ocean waves. *Nature* 297 (1982) 669–671.
4. C. Fox and V. A. Squire, On the oblique reflexion and transmission of ocean waves at shore fast sea ice . *Phil. Trans. R. Soc. London A* 347 (1994) 185–218.
5. C. Fox and V. A. Squire, Reflection and transmission characteristics at the edge of shore fast sea ice. *J. Geophys. Res.* 95 (1990) 11629–11639.
6. C. Fox and V. A. Squire, Strain in shore fast ice due to incoming waves and swell. *J. Geophys. Res.* 96 (1991) 4531–4547.
7. V. A. Squire, Wind over ice: a mechanism for the generation of ice-coupled waves. In: T. K. S. Murthy, J. J. Connor, C. A. Brebbia (eds.), *Proc. 1st Int. Conf. on Ice Technology.* Berlin: Springer-Verlag (1986) 115–128.
8. E. H. Gui and V. A. Squire, Random vibration of floating ice tongues. *Antarc. Sci.* 1 (1989) 157–163.

9. V. A. Squire, W. H. Robinson, M. H. Meylan and T. G. Haskell, Observations of flexural waves on the Erebus Ice Tongue, McMurdo Sound, Antarctica, and nearby sea ice. *J. Glaciol.* 40 (1994) 377–385.
10. C. Fox and H. Chung, Green's function for forcing of a thin floating plate. *Report No. 408,* University of Auckland, N.Z. (1999) 34 pp.
11. C. Fox and V. A. Squire, Coupling between an ocean and an ice shelf. *Ann. Glaciol.* 15 (1991) 101–108.
12. M. H. Meylan and V. A. Squire, The response of ice floes to ocean waves. *J. Geophys. Res.* 99 (1994) 891–900.
13. C. C. Mei, *The Applied Dynamics of Ocean Surface Waves.* Singapore: World Scientific (1994) 740 pp.
14. M. Abramowitz and I. A. Stegun, *Handbook of Mathematical Functions.* New York: Dover (1965) 1046 pp.
15. V. A. Squire and T. W. Dixon, How a region of cracked sea ice affects ice-coupled wave propagation. *Ann. Glaciol.* 33 (In the press).